



Application of direct regularization techniques and bounded-variable least squares for inverse modeling of an urban emissions inventory

Ana Y. Vanoye, Alberto Mendoza

Department of Chemical Engineering, Tecnológico de Monterrey, Ave. Eugenio Garza Sada 2501, Monterrey 64849, Mexico

ABSTRACT

Inverse modeling, coupled with comprehensive air quality models, is being increasingly used for improving spatially and temporally resolved emissions inventories. Of the techniques available to solve the corresponding inverse problem, regularization techniques can provide stable solutions. However, in many instances, it is not clear which regularization parameter selection method should be used in conjunction with a particular regularization technique to get the best results. In this work, three regularization techniques (Tikhonov regularization, truncated singular-value decomposition, and damped singular-value decomposition) and three regularization parameter selection methods (generalized cross validation, the L-curve method (LC), and normalized cumulative periodograms) were applied in conjunction with an air quality model with the aim of identifying the best combination of regularization technique and parameter selection method when using inverse modeling to identify possible flaws in an urban-scale emissions inventory. The bounded-variable least-squares method (BVLS), which is not usually considered a regularization method, was also investigated. The results indicate that the choice of the regularization parameter explains most of the differences between the regularization techniques used, with the LC method exhibiting the best performance for the application described here. The results also show that the BVLS scheme provides the best agreement between the observed and modeled concentrations among the mathematical techniques tested.

Keywords: Air quality model, photochemical modeling, emissions evaluation, inverse problem



Corresponding Author:

Alberto Mendoza

☎ : +52-81-8158-2091

☎ : +52-81-8328-4250

✉ : mendoza.alberto@itesm.mx

Article History:

Received: 08 October 2013

Revised: 19 December 2013

Accepted: 20 December 2013

doi: 10.5094/APR.2014.027

1. Introduction

Three-dimensional comprehensive air quality models (AQMs) describe the atmospheric transport and transformation of trace species and are routinely used in the development of pollution-reduction strategies and other air quality management policies. However, to produce accurate, trustworthy results, AQMs rely on the use of detailed emission inventories that, even today, convey a great degree of uncertainty (Miller et al., 2006; Russell, 2008). This translates into model applications in which discrepancies between model-derived concentrations and observations of air pollutants can be quite large. In this description, we are assuming that the AQM is perfect and the emissions are one of the most uncertain input parameters in the modeling effort (e.g. Russell and Dennis, 2000; Tian et al., 2010).

One way of reducing emission inventory uncertainty is to use inverse modeling or data assimilation techniques to identify possible flaws in the construction of such emission inventories. Applications of inverse modeling range from global (e.g., Petron et al., 2002) or continental (e.g., Elbern et al., 2007) to regional or urban scales (e.g., Quelo et al., 2005) for a variety of atmospheric species such as stratospheric ozone depletion substances (e.g., Xiao et al., 2010), greenhouse gases (e.g., Stohl et al., 2009), radioactive material (e.g., Winiarek et al., 2012), and tropospheric ozone and aerosol precursors (e.g., Gilliland et al., 2006; Napelenok et al., 2008; Henze et al., 2009). In this context, several mathematical techniques have been used to find solutions for the corresponding inverse problems, including four-dimensional data assimilation (e.g., Meirink et al., 2008), Kalman or ensemble Kalman filtering (e.g., Napelenok et al., 2008), and the use of

adjoint models (e.g., Hakami et al., 2005). Li et al. (2010) used genetic algorithms for optimizing inventories, but their application was limited because of the necessary computational requirements.

One approach for performing this top-down emissions inventory evaluation is to first use a forward model (the AQM) to compute both the simulated concentration fields of pollutants and their responses to changes in emissions (sensitivity fields). With this, a linear model of the form $Gm=d$ can be constructed, where d is a vector containing the difference between modeled and observed concentrations, G is a matrix containing the sensitivity coefficients of all pollutant species to changes in the emission strengths, and m is a vector of emission strength changes that brings the observations and model-derived concentrations into agreement. Then, if an over-determined least-squares problem is solved, the corresponding inverse model can be represented as $m^{est}=(G^TG)^{-1}G^Td$, where G^T is the transpose of G . However, inverse problems are typically ill conditioned, and this is an inconvenience because in practice, observations often possess a certain degree of error or noise (Aster et al., 2005).

Several mathematical techniques based on the incorporation of known properties about the solution have been developed with the aim of improving the conditioning of direct inverse problems, including regularization. However, there are few examples of the use of regularization techniques to obtain inverse-derived emissions inventories. In particular, few formal methods have been applied to obtain the value of the regularization parameters. This paper addresses the issue of performing inverse modeling of an urban air-pollutant emission inventory by applying direct regularization techniques. Three regularization techniques and

three regularization parameter choice methods were assessed. An additional technique investigated, which is not usually considered a regularization method, was the bounded-variable least-squares (BVLS) method.

2. Methods

2.1. Regularization methods

Three regularization methods were explored in this work: Tikhonov regularization (TIKH), truncated singular-value decomposition (TSVD), and damped singular-value decomposition (DSVD). Tikhonov's method consists of substituting the least-squares problem for a problem of the form (Neumaier, 1998):

$$m^{est} = \min \left\{ \|Gm - d\|_2 + \|Lm\|_2 \right\} \quad (1)$$

where $L = \lambda I$, I is typically the identity matrix, and $\lambda \in \mathbb{R}$ is a regularization parameter that controls the weight given to the minimization of the additional restriction relative to the minimization of the residual norm. Thus, TIKH seeks a solution that minimizes a criterion made up of the sum of two components: a weighted least-square term and a quadratic penalty term on the solution.

The singular-value decomposition of matrix G with $r = \text{rank}(G)$, as in the following equation:

$$G = USV^T = \sum_{i=1}^r \sigma_i u_i v_i^T \quad (2)$$

can be used to obtain the Moore–Penrose pseudo-inverse of G . However, the generalized inverse solution can become unstable when some of the singular values, σ_i , are small (Aster et al., 2005). Therefore, in TSVD, it is assumed that it is possible to recover a useful model by truncating the sum in Equation (2) in an upper-bound $k < r$ before the smallest singular values start dominating (Hansen, 1990). When $k = r$, the solution of TSVD is identical to the solution obtained by ordinary least-square methods. However, a solution obtained from TSVD with $k < r$ will tend to be more stable (Aster et al., 2005).

In equation (2), U is an orthogonal matrix with columns that are unit basis vectors (u_i) spanning the data space, V is an orthogonal matrix with columns that are basis vectors (v_i) spanning the model space, V^T is the transpose of V , v_i^T is the transpose of v_i , and S is a diagonal matrix with nonnegative diagonal elements (σ_i , the singular values).

Finally, DSVD (Ekstrom and Rhoads, 1974) may be regarded as a regularization method that follows Tikhonov in terms of its TSVD, with the difference being that DSVD introduces a smoother cutoff by means of filter factors that decay slower than the Tikhonov method, overall requiring less filtering (Hansen, 1998; Lin et al., 2011).

2.2. Regularization parameter choice methods

Although the proper choice of the regularization parameter (either the continuous parameter λ or the discrete parameter k) is essential for the effectiveness of the regularization methods applied (Hansen, 1998), the optimal determination of this parameter remains an open issue (Krawczyk–Stando and Rudnicki, 2007; Lin et al., 2011). Some previous studies where inverse modeling has been applied to evaluate emissions inventories have used formal methods to obtain the value of the regularization parameter (Fan et al., 1999; Mendoza–Dominguez and Russell, 2001; Krakauer et al., 2004; Chai et al., 2009; Henze et al., 2009; Saide et al., 2009). However, the strategy of assigning values to the

regularization parameter subjectively, or empirically, prevails (e.g., Eckhardt et al., 2008).

In this study, we explore three methods that do not require a good estimate of the noise variance: generalized cross validation (GCV) (Golub et al., 1979; Haber and Oldenburg, 2000), which is a parameter-choice method based on ordinary cross validation (Allen, 1974); the L-curve method (LC), which uses a plot of the valid regularization parameters of the (semi) norm of the regularized solution versus the corresponding residual norm (the best regularization parameter must be located in the corner of the L-curve) (Hansen and O'Leary, 1993); and normalized cumulative periodograms (NCP) (Rust, 2000; Rust and O'Leary, 2008), which chooses the regularization parameter for which the residual becomes closer to behave as white Gaussian noise.

2.3. Regularization with restrictions

Regardless of whether regularization methods tend to yield more stable, precise solutions, these solutions will often lack physical sense or violate some of the restrictions imposed by the nature of the problem. In our case we need to guarantee positive emissions. Several techniques incorporate additional restrictions to impose boundaries for the solution or add additional information about the solution. One such technique is the BVLS (Stark and Parker, 1995), which solves linear least-squares problems with upper and lower bounds on the variables.

BVLS uses an active set strategy in which the unconstrained least-squares problems for each candidate set of free variables are solved using the QR decomposition. The method also includes a “warm-start” feature that accelerates the solution by allowing for some of the variables to initialize at their upper or lower bounds. Stark and Parker's BVLS algorithm is based on the non-negative least squares method (Lawson and Hanson, 1974).

In this study, we use this additional technique in our application and compare it with the solutions obtained by regularization.

2.4. Application to the GMA emissions inventory

The base case, reported by Mendoza and Garcia (2009), for the modeling of photochemical pollutants in the Guadalajara Metropolitan Area (GMA; 20° 40' 25" N, 103° 20' 38" W) was used as case study. The GMA is the second largest urban center in Mexico, emissions are rather concentrated around the urban core (~600 km²), and no important emission sources are located around this core. In the application described here, the same AQM, spatial configuration of the modeling domain, as well as the same meteorological fields, emissions inventory, and initial and boundary conditions were used. In that study, the California/Carnegie Institute of Technology (CIT) model extended with the capacity of estimating first-order sensitivity coefficients through the direct-decoupled method for three-dimensional models (Yang et al., 1997) was applied for the simulation of a three-day high-ozone concentration episode, occurring from May 16 to May 18, 2001. May was selected for the modeling exercise because it is the month when O₃ concentrations peak in the GMA (Zuk et al., 2007). The modeling domain was a computational matrix composed of 40×40 cells (horizontal resolution), with each cell being 4×4 km and geographically centered in the GMA. In addition, the domain included six vertical levels topping at 3 100 m.

The emission inventory used by Mendoza and Garcia (2009) was based on the 1995 Official Emissions Inventory for the GMA. This inventory had to be extended to provide coverage for the additional municipalities that were included in the modeling domain and that were not part of the GMA. In addition, this inventory had to be scaled from the base year (1995) to the modeled year (2001) and had to be spatially segregated based on

an estimated population density. For this research, it was particularly suitable to have an emission inventory that, given its formulation process, was known to have uncertainties (Mendoza and Garcia, 2011).

Previously, Mendoza and Garcia (2011) used ridge regression (Hoerl and Kennard, 1976) to derive hour-to-hour inverse-modeled emission scaling factors to the emissions for this same application. They found that on a daily average, CO emissions would need to be subject to corrections ranging from –16% to +60%, whereas NO_x and SO₂ emissions would require increments from 100% to 150% and 20% to 140%, respectively. The inverse model proposed by Mendoza and Garcia (2011) notably enhanced the statistical model performance for O₃ and other pollutants predictions; however, several discrepancies among the observed and modeled values remained unsolved.

This new application recreates the original problem, as approached by Mendoza and Garcia (2011), but differs from it in the mathematical methods used. Eight different schemes were tested and compared with the base case and inverse-derived results achieved by Mendoza and Garcia (2011). The schemes were as follows: TIKH combined with GCV, LC, and NCP; DSVD combined with GCV, LC, and NCP; TSVD combined with GCV; and BVLS. The algorithms provided in the Regularization Tools Matlab package, developed by Hansen (2008), were used to perform our numerical experiments. For the BVLS method, a modified version of the original FORTRAN algorithm by Stark and Parker (1995) was used.

The inversion experiments consisted of obtaining correction factors for domain-wide emission of NO_x, CO, and SO₂ using the observational data derived by the eight ground monitoring stations that comprise the routine air quality network of the GMA. Observations of NO, NO₂, CO, SO₂, and O₃ were used in this process. Because the inverse model works under a minimization scheme difference between the observed and simulated values, leaving a residual error that the model cannot explain, and because of the structure of the minimization function, biased estimators are obtained. Therefore, a complete concordance between the observed and modeled values after the inversion process is completed cannot be anticipated. However, a better performance of the AQM may be expected not only for the species directly related to the emissions (i.e., NO, NO₂, CO, and SO₂), but also for the secondary species (e.g., O₃). The inverse-modeling approach, as used here, yielded hourly changes to the original emission inventory that needed to be applied for the AQM to more successfully replicate the observed atmospheric pollutant concentrations. The inversion was conducted under an iterative process due to the non-linear response of some of the constituents (particularly NO, NO₂, and O₃) to the changes in emissions.

Finally, when conducting inverse modeling of emissions, it must be considered that misfits between the model and observations are due to not only emission inaccuracies, but also to errors in meteorological fields and other model parameters, as well as errors in the representation of physical and chemical processes. For this reason, a model evaluation is often required before the inverse-modeling stage (Saide et al., 2009) or these errors must be accounted for by incorporating them into the methodology as an additional term to the minimization function (e.g. Elbern et al., 2007). The corresponding evaluation processes performed for the meteorological and AQMs used in this study were previously described by Mendoza and Garcia (2009). Both models were found to perform within the recommended guidelines for related applications.

3. Results

Table 1 depicts the statistical performance of the base case, that is, the ability of the CIT model to replicate O₃-ambient concentrations. For brevity, only third-day (May 18) simulation results are shown. Table 1 shows the contrasts of that performance with the Mendoza and Garcia (2011) experiment (referred to as the MG test for the remainder of the text) and the eight schemes investigated. The statistical indicators for performance appraisal were those suggested by Doll et al. (1991) for use in AQM applications. Moreover, Tables 2, 3, and 4 show the statistical performance of the AQM for the same day for each of the chemical species whose emissions were directly adjusted by the inverse-modeling process, namely, NO_x, CO, and SO₂, using the previously mentioned inverse-modeling schemes.

As shown in Tables 1 through 4, among the regularization and restricted least squares methods tested, for most performance metrics and for all the chemical species of interest, BVLS consistently performed the best. Particularly, for O₃, Doll et al. (1991) suggest the following performance benchmarks: a normalized bias smaller than ±15%, normalized error smaller than ±35%, and peak estimation accuracy smaller than ±20%. All models tested within these limits, except for the normalized bias, for which only BVLS, DSVD–NCP, and TIKH–NCP yielded satisfactory results.

However, BVLS performance did not always outdo that reported in the MG case, especially concerning O₃ concentrations, but it improved SO₂ significantly [e.g., the daily index of agreement (DIA) increased from 0.48 to 0.52]. CO and NO_x simulations were also enhanced except for the normalized bias, mean normalized square error (MNSE), and root mean square error (RMSE) of NO_x. MNSE is usually regarded as a better metric for spatial and temporal performance appraisal than the normalized error (Hanna, 1988).

Table 1. CIT statistical performance evaluation for simulated O₃ on May 18, 2001^a

	BC	MG	BVLS	DSVD–GCV	DSVD–LC	DSVD–NCP	TIKH–GCV	TIKH–LC	TIKH–NCP	TSVD–GCV
Peak estimation accuracy, %	16.40	–10.20	–6.24	–6.80	–1.66	–4.05	2.23	–1.46	–6.96	3.15
Normalized bias, %	20.30	0.10	11.14	16.61	16.96	13.50	23.54	16.27	7.08	23.79
Normalized error	36.50	15.60	21.41	31.81	26.94	23.01	35.27	26.06	18.81	35.56
MNSE	0.19	0.04	0.05	0.13	0.08	0.06	0.16	0.08	0.04	0.16
RMSE (ppbv)	31.10	21.90	22.65	29.47	24.41	23.36	32.16	24.29	22.95	32.85
RMSE _s (ppbv)	20.70	15.10	14.24	20.98	15.39	15.28	23.55	16.09	16.11	24.56
RMSE _u (ppbv)	23.20	15.80	17.59	20.70	18.94	17.66	21.90	18.20	16.35	21.81
DIA	0.89	0.95	0.95	0.90	0.94	0.94	0.88	0.94	0.94	0.87

^a Statistics were computed by taking into account the residual $r_i = P_i - O_i$, where O_i and P_i are the i^{th} observed and modeled concentrations, respectively. Normalized bias is $1/N \sum (r_i/O_i)$, where N represents the number of valid pairs that originate r_i while the sum runs from $i=1$ to N . In a similar fashion, the normalized error is $1/N \sum [|r_i|/O_i]$, the MNSE is $1/N \sum (r_i/O_i)^2$, and the RMSE is $[1/N \sum (r_i)^2]^{1/2}$. RMSE_s was computed from $[1/N \sum (\hat{r}_i)^2]^{1/2}$, where $\hat{r}_i = \hat{P}_i - O_i$ and $\hat{P}_i = a + bO_i$ (a and b are linear regression coefficients). RMSE follows $\text{RMSE}^2 = \text{RMSE}_s^2 + \text{RMSE}_u^2$. Finally, the DIA is $1 - [N \text{RMSE}^2 / \sum (|P_i - M_o| + |O_i - M_o|)^2]$, where M_o is the mean observed value, as given by $1/N \sum O_i$. Note that a positive bias indicates that modeled values are greater than observed values.

Table 2. CIT statistical performance evaluation for simulated NO_x on May 18, 2001^a

	BC	MG	BVLS	DSVD–GCV	DSVD–LC	DSVD–NCP	TIKH–GCV	TIKH–LC	TIKH–NCP	TSVD–GCV
Normalized bias (%)	–51.10	–13.20	–29.41	–56.84	–32.66	–33.35	–53.77	–35.33	–34.07	–55.90
Normalized error	67.00	61.90	–20.38	69.29	66.04	64.72	68.44	63.26	62.23	69.55
MNSE	2.05	0.83	1.05	2.45	1.15	1.13	2.38	1.18	1.11	2.56
RMSE (ppbv)	43.10	36.70	37.94	44.36	38.65	38.42	44.56	38.46	38.14	45.06
RMSE _s (ppbv)	39.70	26.10	28.14	41.31	29.93	29.23	41.63	30.79	28.69	42.39
RMSE _u (ppbv)	16.90	25.80	25.45	16.16	24.47	24.94	15.89	23.05	25.12	15.30
DIA	0.47	0.59	0.60	0.46	0.58	0.59	0.45	0.58	0.60	0.44

^a Refer to Table 1 for definitions.**Table 3.** CIT statistical performance evaluation for simulated CO on May 18, 2001^a

	BC	MG	BVLS	DSVD–GCV	DSVD–LC	DSVD–NCP	TIKH–GCV	TIKH–LC	TIKH–NCP	TSVD–GCV
Normalized bias (%)	–26.80	–15.60	–15.12	–20.96	–14.88	–15.04	–15.53	–15.21	–15.23	–15.34
Normalized error	60.60	46.20	45.05	45.12	45.29	45.28	45.32	45.31	45.32	45.27
MNSE	0.87	0.44	0.44	0.44	0.44	0.44	0.44	0.44	0.44	0.44
RMSE (ppbv)	1.33	1.05	1.04	1.04	1.04	1.04	1.04	1.04	1.04	1.04
RMSE _s (ppbv)	1.01	0.62	0.64	0.64	0.64	0.64	0.65	0.64	0.64	0.65
RMSE _u (ppbv)	0.86	0.84	0.82	0.82	0.82	0.82	0.82	0.82	0.82	0.82
DIA	0.60	0.76	0.76	0.76	0.76	0.76	0.76	0.76	0.76	0.76

^a Refer to Table 1 for definitions.**Table 4.** CIT statistical performance evaluation for simulated SO₂ on May 18, 2001^a

	BC	MG	BVLS	DSVD–GCV	DSVD–LC	DSVD–NCP	TIKH–GCV	TIKH–LC	TIKH–NCP	TSVD–GCV
Normalized bias (%)	–13.10	10.10	23.85	–16.67	4.41	14.76	–20.51	–10.20	–4.22	–20.25
Normalized error	66.90	79.90	82.35	64.95	69.83	77.22	63.82	64.76	69.60	64.07
MNSE	1.99	1.43	1.11	2.10	1.35	1.26	2.25	1.81	1.70	2.25
RMSE (ppbv)	8.10	7.70	7.26	8.13	7.34	7.44	8.23	7.85	7.89	8.25
RMSE _s (ppbv)	7.30	6.40	5.98	7.43	6.51	6.36	7.58	7.18	7.01	7.57
RMSE _u (ppbv)	3.50	4.20	4.11	3.30	3.37	3.85	3.21	3.16	3.62	3.27
DIA	0.42	0.48	0.52	0.42	0.48	0.47	0.42	0.43	0.43	0.42

^a Refer to Table 1 for definitions.

One of the main differences between regularization methods and BVLS is that the latter restricts the solution to a definite, fixed set of maximum and minimum values, while regularization methods seek a smoother solution. It is possible that BVLS's relatively good performance might be a result of the inventory attributes and that the need of imposing appropriate, plausible bounds was of major concern. This possibility could be explored by performing further experiments with other inventories.

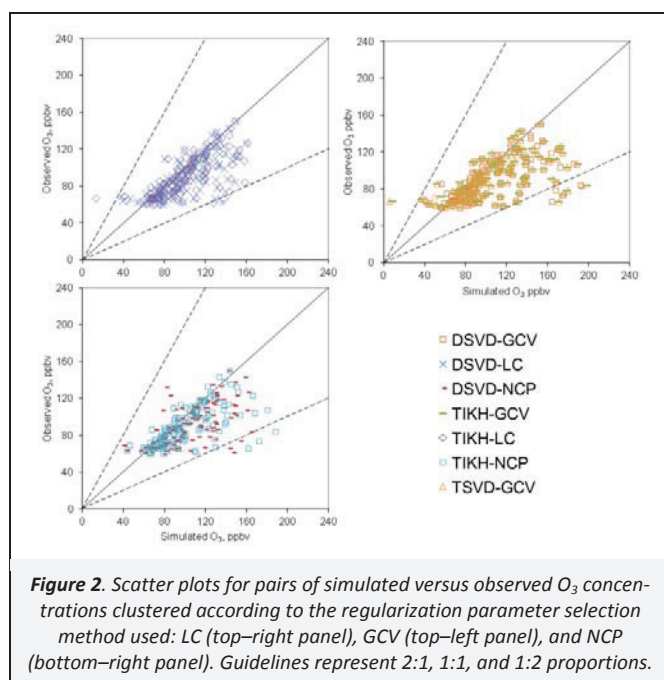
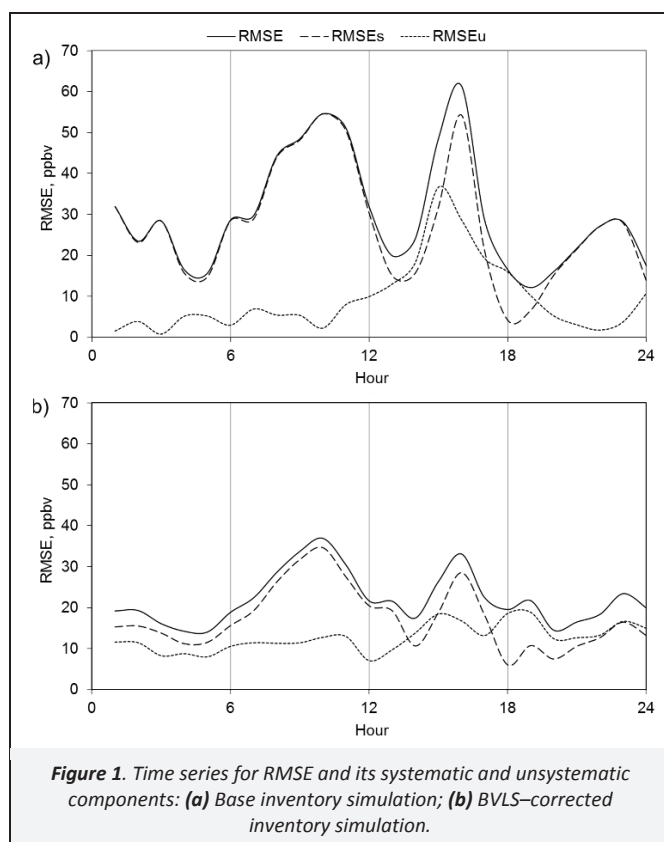
All methods generally showed lower RMSE when compared with the base case. However, it is important to also assess the relative weights of the systematic (RMSE_s) and unsystematic (RMSE_u) components of the RMSE. In this context, the regularization schemes tested yielded mixed results. In all NO_x and SO₂ simulations, RMSE_s prevailed over RMSE_u, whereas for the CO results, RMSE_u outweighed its systematic counterpart. O₃ showed a mixed response: only BVLS and those simulations using LC and NCP parameter choice schemes presented higher RMSE_u than RMSE_s, indicating that in such applications, residual errors are mostly caused by variations (noise) that the forward model cannot resolve.

Time series for the RMSE statistic were also explored with the aim of determining whether the CIT was adequately simulating the temporal dynamics of O₃. For the BVLS run, Figure 1 shows the time evolution of RMSE, RMSE_s, and RMSE_u. It should be noted that overall, RMSE diminished at all hours compared with the base case simulation. Furthermore, as was also reported in the MG case, there appears to be a local minimum in the RMSE during the

afternoon hours. This might be a result of the fact that the CIT, as other photochemical air quality models, has been partially calibrated (tuned) to perform best under conditions where O₃ levels are the highest as O₃ peaks are of more environmental concern than low concentrations (Russell and Dennis, 2000). However, the mere presence of RMSE_s indicates that the model requires further improvement for better results.

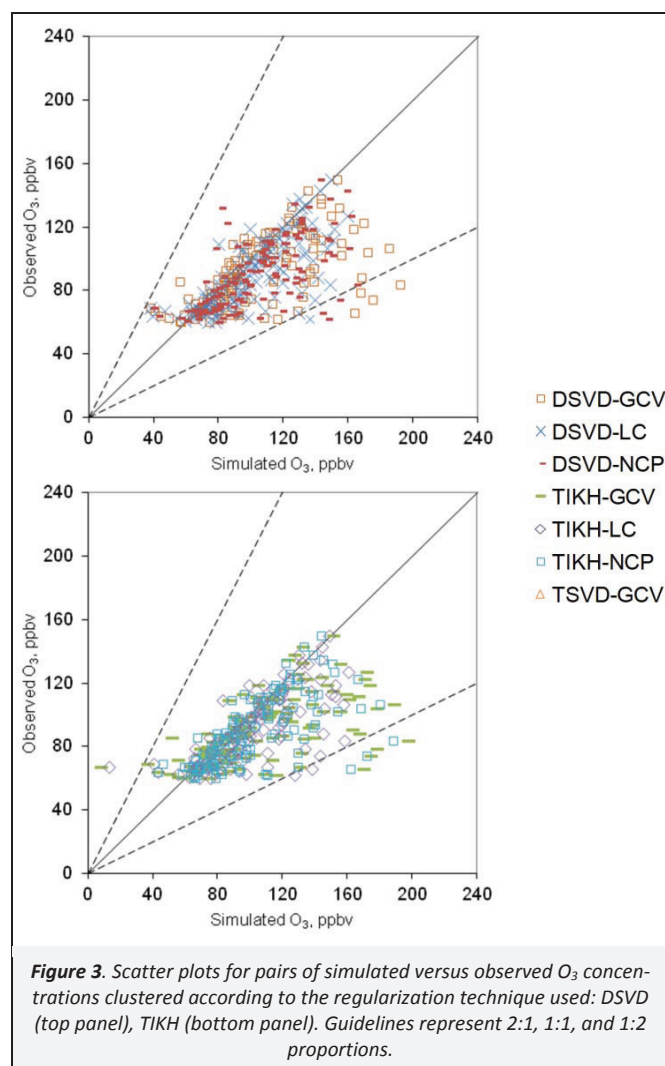
Because different combinations of regularization techniques and parameter selection methods were assessed, it became evident that it would be useful to evaluate the relative impact of the choice of regularization technique versus the choice of the regularization parameter method. Thus, the results were segregated into clusters of simulations using the same regularization method and the same regularization parameter selection method. Dispersion plots were constructed by pairing observed and simulated species concentrations. Linear regression models were fitted to each of the proposed combinations, which revealed that the use of the same regularization parameter selection method explained most of the variance shown among the different tested schemes. Figure 2 depicts the model response for O₃ using the different regularization parameter selection methods, and Figure 3 presents the model's response for O₃ using different regularization methods. Correlation (R^2) values for regularization schemes using LC were between 0.517 and 0.522, whereas regularization schemes using NCP or GCV for parameter selection ranged between 0.414 and 0.416 and 0.370 and 0.377, respectively. When assembling the results by regularization method (e.g., DSVD or TIKH), DSVD-based methods yielded R^2 values between 0.370 and 0.522, whereas

TIKH-based methods yielded values ranging from 0.374 to 0.517. From this analysis, it became clear that R^2 values were more sensitive to changes in the choice of the regularization parameter, regardless of the accompanying regularization method, than to the choice of the regularization method per se.



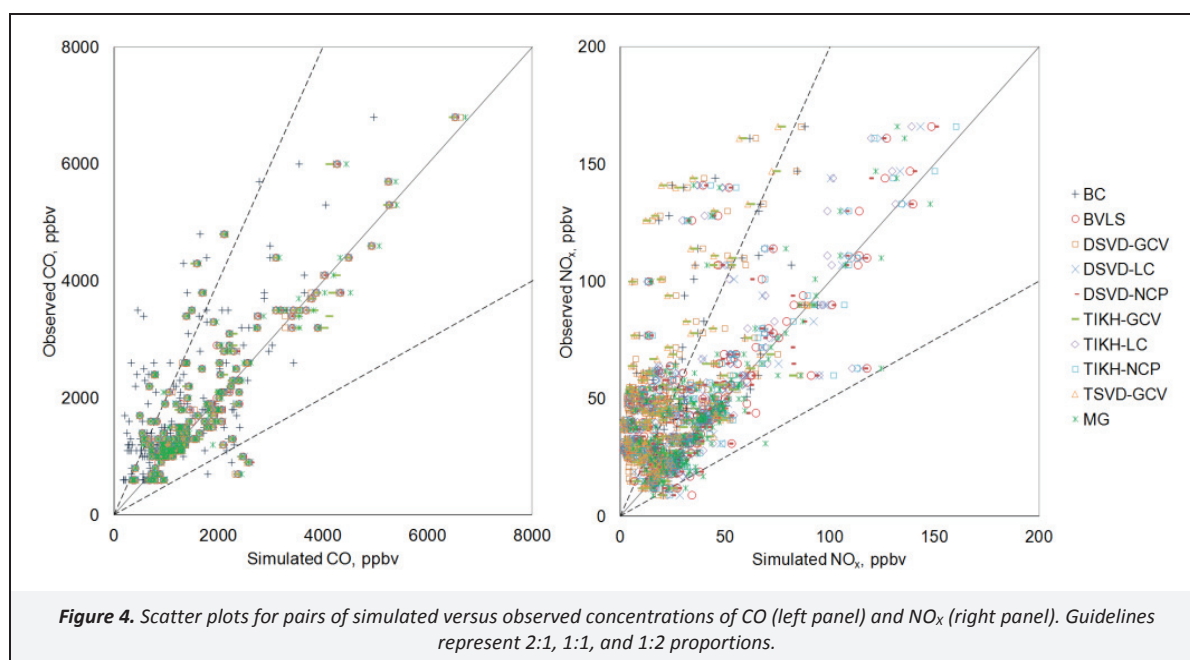
Whereas special emphasis has been put on the adequate modeling of ambient O_3 concentrations because of its possible adverse effects on human health and non-linear nature, dispersion plots were also constructed for the species NO_x and CO (Figure 4). For these species, as for O_3 , most of the regularization methods showed similar behavior among them. This likeness was

remarkably evident for CO, as can be seen in Table 3. However, as previously shown, differences arose depending on the choice of regularization parameter selection method. For this particular application, the regularization schemes using the LC method demonstrated better performance than the rest of the schemes.



In this study, the correction of NO_x emissions was relevant because within urban environments, O_3 is mostly produced by photochemical reactions between NO_x and volatile organic compounds (VOCs), which explains the high correlation shown by NO_x and O_3 performance metrics for all test runs. That is, correcting the emissions of primary species (NO_x) leads to the automatic improvement in the estimation of secondary species. However, VOC emissions were not corrected because of a lack of proper observations to constrain their inversion. Thus, the remaining differences could be attributed to uncertain VOC emissions.

Finally, after analyzing the behavior of SO_2 , it was concluded that this model application, even after undergoing regularization processes, was unable to adequately reproduce the observed SO_2 concentrations within the GMA (Table 4). In this regard, it is believed that the level of uncertainty in current SO_2 emission inventories is still large enough as to overcome any effort aimed at correcting these emissions via mathematical regularization methods. Thus, the spatial distribution of these emissions would need to be revised through a down-top methodology.



In addition to the combinations among regularization methods and regularization parameter–selection methods described above, further combinations are possible. For example, initial exploration of TSVD–LC and TSVD–NCP was conducted. However, they were not further analyzed because similar conclusions on the relevance of the regularization parameter selection method over the regularization technique could be drawn from those initial tests.

5. Conclusions

Inverse modeling is being increasingly used as a top–down analysis tool for emissions inventory assessment. In particular, regularization is a mathematical technique that provides numerical stability for this type of ill–conditioned problem and, thus, was explored in this investigation. A common feature to all regularization techniques is that they require the selection of a regularization parameter that seeks to balance the minimization error and the regularization error. In addition, there are restricted least–squares methodologies that solve the inverse problem by restraining the solution to a specific set of boundaries (e.g., BVLS).

In this work, several regularization schemes and one restricted least–squares method were tested and compared using statistical performance criteria with the MG test (2011). This experiment consisted of detecting possible improvements in the emission inventory of ozone precursors at the scale of an urban center (Guadalajara, Mexico, in this case). Overall, the BVLS consistently showed the best agreement among the other mathematical techniques tested. In addition, regularization methods demonstrated almost indistinct behavior patterns among them. Nonetheless, the choice of the regularization parameter was found to explain most of the variance shown among the different tested schemes, with the techniques using the LC method exhibiting better agreement between the observed and simulated values than their NCP and GCV counterparts.

Acknowledgements

This work was supported by Tecnológico de Monterrey through grant No. 0020CAT186. A.Y. Vanoye further acknowledges the support (scholarship) received from Mexico's National Council for Science and Technology (CONACYT) during her research stay at Tecnológico de Monterrey.

References

- Allen, D.M., 1974. The relationship between variable selection and data augmentation and a method for prediction. *Technometrics* 16, 125–127.
- Aster, R.C., Borchers, B., Thurber, C.H., 2005. *Parameter Estimation and Inverse Problems*, Elsevier Academic Press, Burlington, pp. 89–118.
- Chai, T.F., Carmichael, G.R., Tang, Y.H., Sandu, A., Heckel, A., Richter, A., Burrows, J.P., 2009. Regional NO_x emission inversion through a four–dimensional variational approach using SCIAMACHY tropospheric NO₂ column observations. *Atmospheric Environment* 43, 5046–5055.
- Doll, D.C., Scheffe, R.D., Meyer, E.L., Chu, S.–H., 1991. Guideline for Regulatory Application of the Urban Airshed Model, EPA–450/4–91–013, Office of Air Quality, Planning and Standards, United States Environmental Protection Agency, Research Triangle Park, 89 pages.
- Eckhardt, S., Prata, A.J., Seibert, P., Stebel, K., Stohl, A., 2008. Estimation of the vertical profile of sulfur dioxide injection into the atmosphere by a volcanic eruption using satellite column measurements and inverse transport modeling. *Atmospheric Chemistry and Physics* 8, 3881–3897.
- Ekstrom, M.P., Rhoads, R.L., 1974. On the application of eigenvector expansions to numerical deconvolution. *Journal of Computational Physics* 14, 319–340.
- Elbern, H., Strunk, A., Schmidt, H., Talagrand, O., 2007. Emission rate and chemical state estimation by 4–dimensional variational inversion. *Atmospheric Chemistry and Physics* 7, 3749–3769.
- Fan, S.M., Sarmiento, J.L., Gloor, M., Pacala, S.W., 1999. On the use of regularization techniques in the inverse modeling of atmospheric carbon dioxide. *Journal of Geophysical Research–Atmospheres* 104, 21503–21512.
- Gilliland, A.B., Appel, K.W., Pinder, R.W., Dennis, R.L., 2006. Seasonal NH₃ emissions for the continental united states: Inverse model estimation and evaluation. *Atmospheric Environment* 40, 4986–4998.
- Golub, G.H., Heath, M., Wahba, G., 1979. Generalized cross–validation as a method for choosing a good ridge parameter. *Technometrics* 21, 215–223.
- Haber, E., Oldenburg, D., 2000. A GCV based method for nonlinear ill–posed problems. *Computational Geosciences* 4, 41–63.
- Hakami, A., Henze, D.K., Seinfeld, J.H., Chai, T., Tang, Y., Carmichael, G.R., Sandu, A., 2005. Adjoint inverse modeling of black carbon during the Asian Pacific Regional Aerosol Characterization Experiment. *Journal of Geophysical Research–Atmospheres* 110, art. no. D14301.

- Hannna, S.R., 1988. Air-quality model evaluation and uncertainty. *JAPCA–The International Journal of Air Pollution Control and Hazardous Waste Management* 38, 406–412.
- Hansen, P.C., 2008. Regularization Tools. A Matlab Package for Analysis and Solution of Discrete Ill-Posed Problems, Version 4.1 for Matlab 7.4, Technical University of Denmark, pp. 13–42.
- Hansen, P.C. 1998. *Rank-Deficient and Discrete Ill-Posed Problems*, Society for Industrial and Applied Mathematics, Philadelphia, pp. 99–131.
- Hansen, P.C., 1990. Truncated singular value decomposition solutions to discrete ill-posed problems with ill-determined numerical rank. *SIAM Journal on Scientific and Statistical Computing* 11, 503–518.
- Hansen, P., O'Leary, D., 1993. The use of the L-curve in the regularization of discrete ill-posed problems. *SIAM Journal on Scientific Computing* 14, 1487–1503.
- Henze, D.K., Seinfeld, J.H., Shindell, D.T., 2009. Inverse modeling and mapping US air quality influences of inorganic PM_{2.5} precursor emissions using the adjoint of GEOS-Chem. *Atmospheric Chemistry and Physics* 9, 5877–5903.
- Hoerl, A.E., Kennard, R.W., 1976. Ridge regression iterative estimation of the biasing parameter. *Communications in Statistics-Theory and Methods* 5, 77–88.
- Krakauer, N.Y., Schneider, T., Randerson, J.T., Olsen, S.C., 2004. Using generalized cross-validation to select parameters in inversions for regional carbon fluxes. *Geophysical Research Letters* 31, art. no. L19108.
- Krawczyk-Stando, D., Rudnicki, M., 2007. Regularization parameter selection in discrete ill-posed problems – the use of the U-curve. *International Journal of Applied Mathematics and Computer Science* 17, 157–164.
- Lawson, C.W., Hanson, R.J., 1974. *Solving Least Squares Problems*, John Wiley and Sons, New York, pp. 350.
- Li, M.J., Chen, D.S., Cheng, S.Y., Wang, F., Li, Y., Zhou, Y., Lang, J.L., 2010. Optimizing emission inventory for chemical transport models by using genetic algorithm. *Atmospheric Environment* 44, 3926–3934.
- Lin, J., Chen, W., Wang, F.Z., 2011. A new investigation into regularization techniques for the method of fundamental solutions. *Mathematics and Computers in Simulation* 81, 1144–1152.
- Meirink, J.F., Bergamaschi, P., Krol, M.C., 2008. Four-dimensional variational data assimilation for inverse modelling of atmospheric methane emissions: Method and comparison with synthesis inversion. *Atmospheric Chemistry and Physics* 8, 6341–6353.
- Mendoza, A., Garcia, M.R., 2011. Inverse modeling applied to the analysis of emission inventory of the metropolitan area of Guadalajara, Mexico. *Revista Internacional de Contaminación Ambiental* 27, 199–214.
- Mendoza, A., Garcia, M.R., 2009. Implementation of an air quality model of second generation to the metropolitan area of Guadalajara, Mexico. *Revista Internacional de Contaminación Ambiental* 25, 73–85.
- Mendoza-Dominguez, A., Russell, A.G., 2001. Emission strength validation using four-dimensional data assimilation: Application to primary aerosol and precursors to ozone and secondary aerosol. *Journal of the Air & Waste Management Association* 51, 1538–1550.
- Miller, C.A., Hidy, G., Hales, J., Kolb, C.E., Werner, A.S., Haneke, B., Parrish, D., Frey, H.C., Rojas-Bracho, L., Deslauriers, M., Pennell, B., Mobley, J.D., 2006. Air emission inventories in North America: A critical assessment. *Journal of the Air & Waste Management Association* 56, 1115–1129.
- Napelenok, S.L., Pinder, R.W., Gilliland, A.B., Martin, R.V., 2008. A method for evaluating spatially-resolved NO_x emissions using Kalman filter inversion, direct sensitivities, and space-based NO₂ observations. *Atmospheric Chemistry and Physics* 8, 5603–5614.
- Neumaier, A., 1998. Solving ill-conditioned and singular linear systems: A tutorial on regularization. *SIAM Review* 40, 636–666.
- Petron, G., Granier, C., Khattatov, B., Lamarque, J.F., Yudin, V., Muller, J.F., Gille, J., 2002. Inverse modeling of carbon monoxide surface emissions using Climate Monitoring and Diagnostics Laboratory network observations. *Journal of Geophysical Research–Atmospheres* 107, art. no. 4761.
- Quelo, D., Mallet, V., Sportisse, B., 2005. Inverse modeling of NO_x emissions at regional scale over northern France: Preliminary investigation of the second-order sensitivity. *Journal of Geophysical Research–Atmospheres* 110, art. no. D24310.
- Russell, A.G., 2008. EPA Supersites Program-related emissions-based particulate matter modeling: Initial applications and advances. *Journal of the Air & Waste Management Association* 58, 289–302.
- Russell, A., Dennis, R., 2000. NARSTO critical review of photochemical models and modeling. *Atmospheric Environment* 34, 2283–2324.
- Rust, B.W., 2000. Parameter selection for constrained solutions to ill-posed problems. *Computing Science and Statistics* 32, 333–347.
- Rust, B.W., O'Leary, D.P., 2008. Residual periodograms for choosing regularization parameters for ill-posed problems. *Inverse Problems* 24, art. no. 034005.
- Saide, P., Osses, A., Gallardo, L., Osses, M., 2009. Adjoint inverse modeling of a CO emission inventory at the city scale: Santiago de Chile's case. *Atmospheric Chemistry and Physics Discussion* 9, 6325–6361.
- Stark, P.B., Parker, R.L., 1995. Bounded-variable least-squares – an algorithm and applications. *Computational Statistics* 10, 129–141.
- Stohl, A., Seibert, P., Arduini, J., Eckhardt, S., Fraser, P., Grealley, B.R., Lunder, C., Maione, M., Muhle, J., O'Doherty, S., Prinn, R.G., Reimann, S., Saito, T., Schmidbauer, N., Simmonds, P.G., Vollmer, M.K., Weiss, R.F., Yokouchi, Y., 2009. An analytical inversion method for determining regional and global emissions of greenhouse gases: Sensitivity studies and application to halocarbons. *Atmospheric Chemistry and Physics* 9, 1597–1620.
- Tian, D., Cohan, D.S., Napelenok, S., Bergin, M., Hu, Y.T., Chang, M., Russell, A.G., 2010. Uncertainty analysis of ozone formation and response to emission controls using higher-order sensitivities. *Journal of the Air & Waste Management Association* 60, 797–804.
- Winiarek, V., Bocquet, M., Saunier, O., Mathieu, A., 2012. Estimation of errors in the inverse modeling of accidental release of atmospheric pollutant: Application to the reconstruction of the cesium-137 and iodine-131 source terms from the Fukushima Daiichi power plant. *Journal of Geophysical Research–Atmospheres* 117, art. no. D05122.
- Xiao, X., Prinn, R.G., Fraser, P.J., Weiss, R.F., Simmonds, P.G., O'Doherty, S., Miller, B.R., Salameh, P.K., Harth, C.M., Krummel, P.B., Golombek, A., Porter, L.W., Butler, J.H., Elkins, J.W., Dutton, G.S., Hall, B.D., Steele, L.P., Wang, R.H.J., Cunnold, D.M., 2010. Atmospheric three-dimensional inverse modeling of regional industrial emissions and global oceanic uptake of carbon tetrachloride. *Atmospheric Chemistry and Physics* 10, 10421–10434.
- Yang, Y.J., Wilkinson, J.G., Russell, A.G., 1997. Fast, direct sensitivity analysis of multidimensional photochemical models. *Environmental Science & Technology* 31, 2859–2868.
- Zuk, M., Rojas Bracho, L., Tzintzun Cervantes, M.G., 2007. *Third almanac of air quality data and tendencies in nine Mexican cities*, National Institute of Ecology, Mexico, pp. 116 (in Mexican).